6285,

Litten 1889

Draft Okt. 2005

Determination of a Gravity Field Model from one Month of CHAMP Satellite Data using Accelerations

Tin Lian Abt, *Institute of Geodesy, University of Stuttgart, Germany*
Eva Howe, *Department of Geophysics, University of Copenhagen, Denmark*
Carl Christian Tscherning, *Department of Geophysics, University of Copenhagen, Denmark*

ABSTRACT

A gravity field model has been estimated based on reduced dynamic and kinematic state vectors of CHAMP. Newton Interpolation has been used to calculate accelerations and Least-Squares Collocation to estimate the spherical harmonic coefficients.

During data preprocessing positions and velocities of the reduced dynamic and kinematic state vectors are synchronised so that two corresponding data sets of one month (July 2002) with a sampling rate of 30s are achieved. Observations where the kinematic velocity is rejected due to edge effects or GPS observation discontinuities are deleted in both data sets.

A comparison of the two sets of state vectors shows that the majority of the differences in magnitude of position and velocity are in the range between ±0.2m and ±0.5mm/s respectively. Observations outside these boundaries are declared outliers and deleted. This reduces the data sets by approximately 0.7%.

Newton Interpolation approximates the velocity vectors which are transformed into an inertial system by a polynomial. Tests ascertain that the use of seven ~~interpolation-points~~ achieves good results. The first derivative with respect to time of these polynomials gives the acceleration vector of each observation.

One-third of the reduced dynamic and kinematic observations have been utilised for the estimation of spherical harmonic coefficients. The Least-Squares Collocation method was used with ~~is based on~~ gravity disturbances derived from the magnitudes of accelerations as input data. EGM96 up to a degree and order of 24 is used in the ~~for the~~ "remove-restore" procedure ~~method~~ so that residual data become statistically more homogenised.

A comparison of the reduced dynamic and kinematic accelerations to those based on EGM96 up to a degree and order of 360 shows that the kinematic data are more influenced by noise than the reduced dynamic. The standard deviations of differences in accelerations calculated from EGM96 minus reduced dynamic or kinematic are 0.3mgal and 1mgal respectively.

These results are also reflected in the quality of the spherical harmonic coefficients. The standard deviations of differences in coefficients between EGM96 and reduced dynamic data are always lower than those between EGM96 and kinematic data.

Up to degree 60, both types of standard deviations are lower than the standard deviations of EGM96 coefficients themselves. The estimated gravity field model therefore provides information consistent with EGM96 up to degree 60. The model shows also an improvement with respect to coefficients which are derived by the energy conservation method utilising the same data.

INTRODUCTION

Geosciences have the aim to create a global model of the earth which leads to a better understanding of its structure and composition. This understanding refers to a planet not only being static but also being a dynamic system that varies over time. The global gravity field forms in this context one of the most fundamental parameters.

Former gravity field models have been obtained from a combination of satellite tracking data, local terrestrial gravity measurements and satellite altimetry data.
In order to improve these models three different satellite missions have been designed, CHAMP, GRACE and GOCE. They all have in common a low earth orbiting satellite. Due to the low altitude the accuracy and resolution of existing gravity field models can be increased. The ~~three satellite missions have also the advantage~~ that they each cover almost the whole earth so that problems of combining different satellite tracking data sets are dissolved.

This

With~~in~~ ~~the described~~ background, the task of this study is the computation of a gravity field model. Furthermore, this gravity field model should be based on the accelerations of the low orbiting CHAMP satellite.

DATA SETS OF CHAMP MEASUREMENTS

Via satellite-to-satellite tracking, a GPS receiver continuously monitors the orbit of the CHAMP satellite. Perturbations of this orbit indicate varying gravity.

channels

Within this research two different sets of CHAMP data have been used, *reduced dynamic* and *kinematic*, both containing the measurements ~~of~~ July 2002. The *reduced dynamic* state vectors were obtained from GFZ Potsdam while the *kinematic* state vectors were kindly provided by Lorant Földvary at IAPG of the Technical University of Munich.

The time interval for *kinematic* and *reduced dynamic* observations are 30s and 10s respectively hence the *reduced dynamic* observations are able to represent the orbit of the satellite in more details.

In order to benefit from both observation methods ~~it is~~ recommended to use both data sets. If these sets are compared to each other it will be possible to decide whether certain observations are likely to be more accurate or not. Errors can be detected more easily if there are two sources for each state vector. However, a synchronisation of the two data sets has to be carried out before they can be compared to each other.

In order to analyse corresponding observations of the same time step, the type of data and the time frames of both data sets have to be the same. For this reason, the days in the *reduced dynamic* data set which are given as Julian days since J2000.0 are converted into days of the month as given by the *kinematic* orbit format. While the *kinematic* orbit is observed in GPS Time (GPST) the *reduced dynamic* observations are given in Terrestrial Time (TT). Both time frames can easily be transformed into the common civil time Coordinated Universal Time (UTC) by equation 1 and equation 2.

$$UTC = GPST - 13\,s \tag{1}$$

$$UTC = TT - 64.148\,s \tag{2}$$

As the *reduced dynamic* data sampling rate is three times higher than the *kinematic* data sampling rate (10s versus 30s) no more than one third of the *reduced dynamic* observations can be taken.

Some gaps occur within the *reduced dynamic* data set and not all *kinematic* can be utilised due to GPS observation discontinuities and edge effects. Only measurements of one data set which have a corresponding measurement in the other data set are selected for further investigations.

The differences in position and velocity of the synchronised data are presented in figure 1 and figure 2.

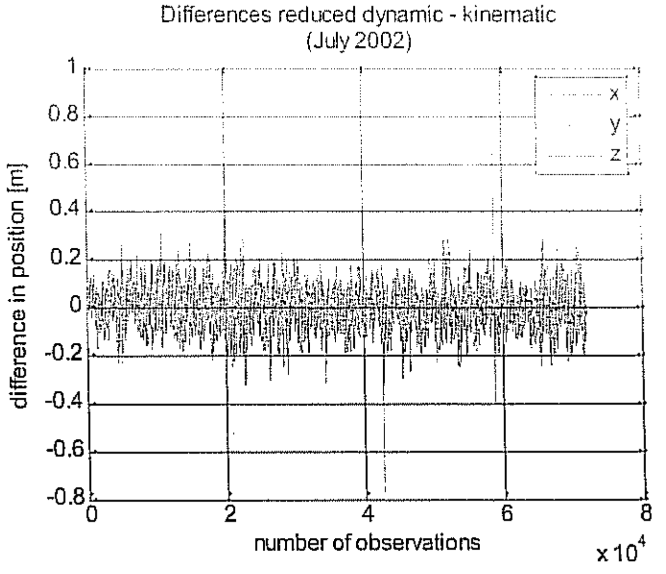

figure 1: differences in position (July 2002)

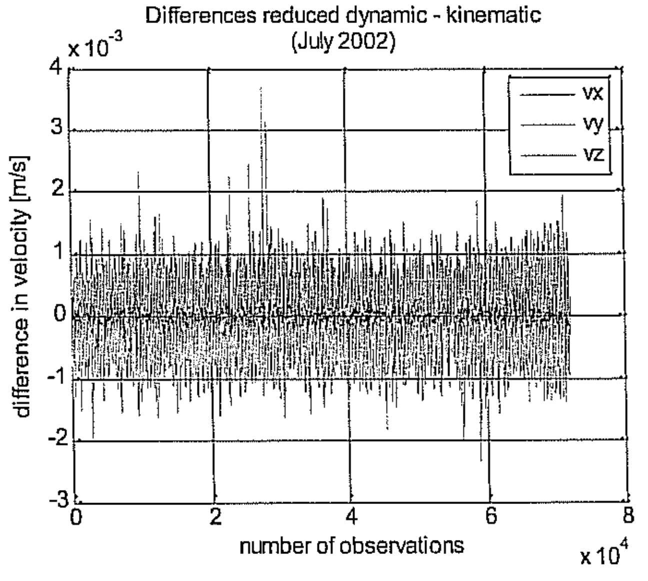

figure 2: differences in velocity (July 2002)

The differences are each time plotted over a period of one month. The three graphs represent the differences with respect to the coordinate axes x, y and z. According to figure 1, it strikes that the z component which is the most interesting one because it gives the height of the satellite seems also to be the most stable one. There are not such big extremes as occur in the x and y component.

As mentioned earlier, the advantage of two different data sets is that errors can be detected more easily. For that reason the magnitudes of the position and velocity vectors of the *reduced dynamic* and *kinematic* observations are compared. The differences are presented in figure 3 and figure 4.

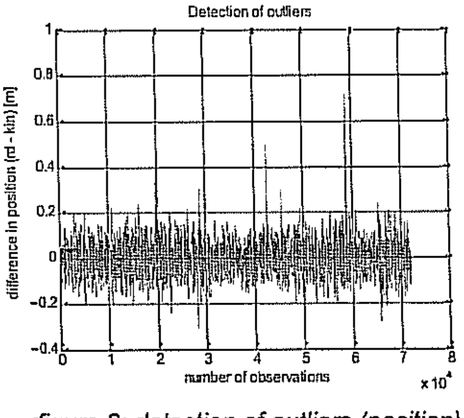

figure 3: detection of outliers (position)

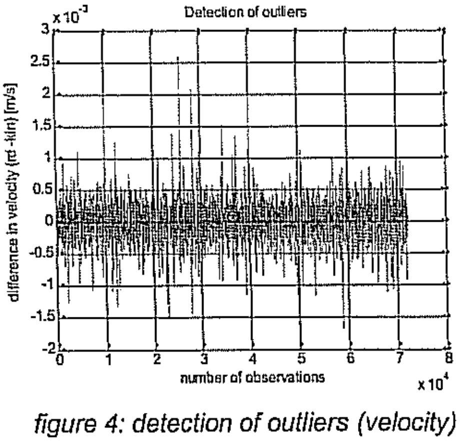

figure 4: detection of outliers (velocity)

From the above figures, the conclusion can be drawn that the majority of differences in position occur between -0.2m and +0.2m while most of the differences in velocity occur between -0.5mm/s and +0.5mm/s. Observations which lie outside these boundaries are declared outliers and deleted.

A higher difference at one point may indicate an error or a discontinuity in at least one of the two data files at that point. If those outliers are filtered, a more accurate set of data can be achieved. Around 500 out of 72,000 observations in each data set are declared outliers reducing the data sets by 0.7%.

COMPUTATION OF ACCELERATIONS

A common way of deriving accelerations is to compute either the second derivative of the observed positions or the first derivative of the velocities. A more sophisticated approach is the interpolation through several observations.

A seven-point Newton Interpolation is therefore utilised to describe the CHAMP orbit [Austen and Reubelt 2000]. The below polynomial (equation 3) approximates the point-wise velocities as a continuous function in case of equidistant observations.

$$V(t) = V_0 + \sum_{i=1}^{n} \Delta_{i/2}^{i} = V_0 + \binom{s}{1}\Delta_{1/2}^{1} + \binom{s}{2}\Delta_{1}^{2} + \binom{s}{3}\Delta_{3/2}^{3} + \cdots + \binom{s}{n}\Delta_{n/2}^{n} \qquad (3)$$

$$with \quad s = \frac{t}{\Delta t}$$

The parameter s will always be constant due to a constant sampling rate. In case of the seven-point interpolation s equals three while t represents the time.

The vector Δ includes the differences of the velocity vectors V according to the difference scheme of equidistant observations (equation 4).

$$\Delta_{n/2}^{n} = \sum_{i=0}^{n} (-1)^{n+1} \binom{n}{i} X_i \qquad (4)$$

The first derivative of the polynomial in equation 3 finally delivers the accelerations in equation 5.

$$\dot{V}(t) = \binom{s}{1}' \Delta_{1/2}{}^{1} + \binom{s}{2}' \Delta_{1}{}^{2} + \binom{s}{3}' \Delta_{3/2}{}^{3} + \cdots + \binom{s}{n}' \Delta_{n/2}{}^{n}$$
$$= \frac{1}{\Delta t} \left\{ \Delta^{1}_{1/2} + \frac{2s-1}{2!} \Delta^{2}_{1} + \frac{3s^2-6s+2}{3!} \Delta^{3}_{3/2} + \cdots + \frac{1}{n!} \sum_{k=0}^{n-1} \frac{\prod_{i=0}^{n-1} (s-i)}{s-k} \Delta^{n}_{n/2} \right\} \tag{5}$$

Those calculations are carried out in an inertial reference system requiring a transformation of the CHAMP state vectors.

ESTIMATION OF SPHERICAL HARMONIC COEFFICIENTS

A gravity field is expressed by its spherical harmonic coefficients c_{ij} and s_{ij}. Those coefficients are here derived by using Least-Squares Collocation (equation 6). The anomalous potential T in an arbitrary point P is thereby approximated by the observations *obs* and their covariances *cov* (equation 7) [Tscherning 2001]. In this case the observations are gravity disturbances which are based on the above accelerations (equation 5).

$$\frac{GM}{a} \begin{Bmatrix} c_{ij} \\ s_{ij} \end{Bmatrix} \tag{6}$$
$$= \frac{1}{4\pi} \iint_{\varphi=-\frac{\pi}{2}\ \lambda=0}^{\frac{\pi}{2}\ 2\pi} \bar{P}_{ij}(\sin(\varphi_p))\, T(P) \begin{Bmatrix} \cos(j\lambda_p) \\ \sin(j\lambda_p) \end{Bmatrix} \cos(\varphi_p)\, d\lambda\, d\varphi \quad \begin{matrix} if\ \ j \geqslant 0 \\ if\ \ j < 0 \end{matrix}$$

$$\begin{aligned} \hat{T}(P) &= \sum_{k=1}^{N} b_k\, cov(T(P), obs_k) \\ with \quad \{b_i\} &= \{cov(i,j)\}^{-1} \{obs_j\} \end{aligned} \tag{7}$$

The index N stands for the number of measurements while the elements b_k are the solutions of the normal equations and are constant.

The errors E of the spherical harmonic coefficients can be estimated by equation 8 with $C0$ being the autocovariances of the coefficients and $cov(i,j)$ being the normal equation matrix.

$$\boldsymbol{E}^2 = \boldsymbol{C}_0 - \{cov(\frac{GM}{a}c_{ij}, obs_k)\}^T \{cov(i,j)\}^{-1} \{cov(\frac{GM}{a}c_{ij}, obs_k)\} \qquad (8)$$

The presented Least-Squares Collocation is implemented in the GRAVSOFT [Tscherning et al. 1994] program GEOCOL [Tscherning 1974] which is written in FORTRAN.

magnitude of the The computation

Only one-third of the synchronised and filtered data haven been used during collocation in order to reduce the system of normal equations. This leads to a distribution of observations as shown in figure 5.

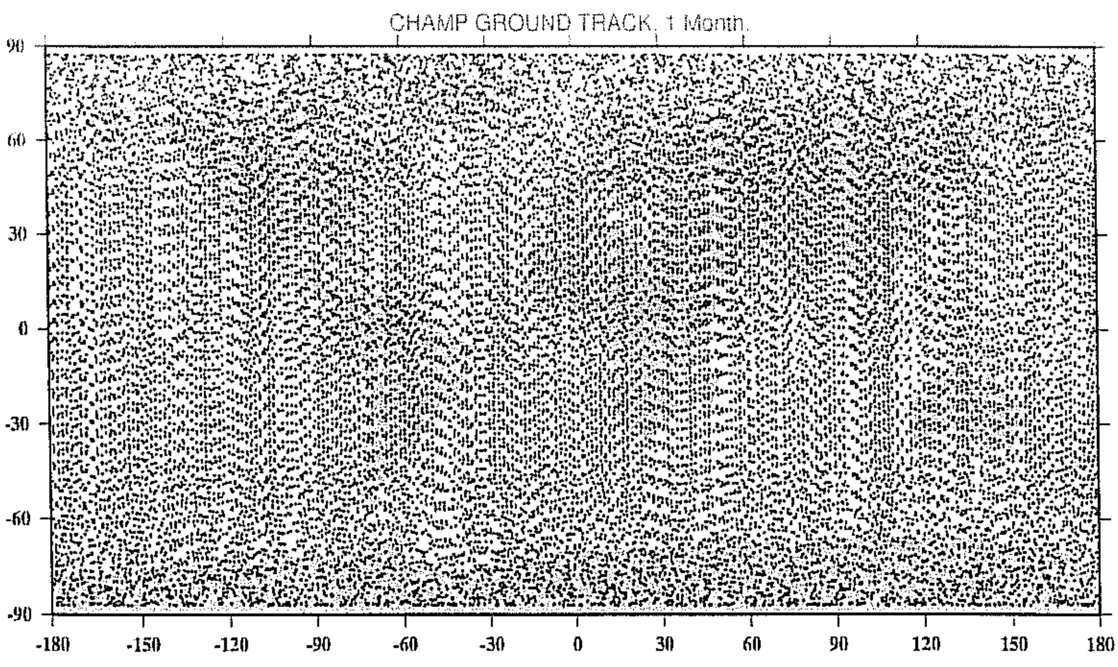

figure 5: ground tracks (method one)

RESULTS

This section discusses the results that have been derived for the three categories: accelerations, gravity disturbances and spherical harmonic coefficients.

Accelerations

After the accelerations were derived from the *reduced dynamic* and *kinematic* velocities, it is interesting to find out how well they fit to a reference model. EGM96 is chosen as the reference model [Lemoine et al. 1998].

The *reduced dynamic* and *kinematic* magnitudes of accelerations are subtracted from those accelerations which are derived from EGM96. The maximum, minimum, mean and standard deviation of the differences that occur within July 2002 are shown in table 1 (*reduced dynamic*) and table 2 (*kinematic*).

table 1

Differences in acceleration [m/s^2] (EGM96 – reduced dynamic)

max	*min*	*mean*	*std*
2.589e-05	-1.632e-05	-7.144e-08	3.169e-06

table 2

Differences in acceleration [m/s^2] (EGM96 – kinematic)

max	*min*	*mean*	*std*
8.368e-05	-8.933e-05	-8.077e-08	1.038e-05

The majority of the differences in both cases are of size $10^{-5} m/s^2$, i.e. around a few mgals. The *reduced dynamic* accelerations are more consistent with ~~to~~ EGM96 than the *kinematic* although *reduced dynamic* and *kinematic* differences have similar sizes. This is supported by the differences in standard deviations (0.3mgal versus 1mgal) which emphasises that the *reduced dynamic* data are slightly more accurate than the *kinematic*.

The above calculated differences are plotted in figure 6. Here, the same conclusions are drawn as before. The *reduced dynamic* accelerations (red) show smaller amplitudes, that means these accelerations have less differences to EGM96 than the *kinematic* accelerations (blue).

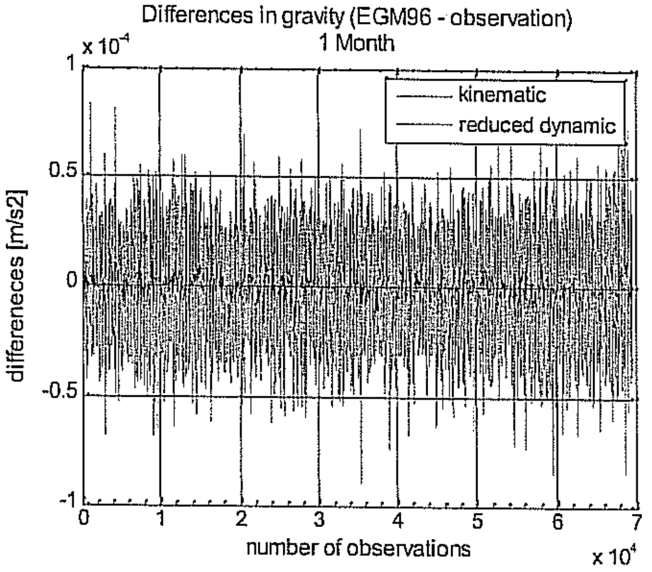

figure 6: differences in gravity

The main problem of the *kinematic* data is probably that the GPS measurements cause too much noise. As a result, an orbit described by the *reduced dynamic* data becomes smoother than the *kinematic* orbit.

Nevertheless, both data sets are used to derive a gravity field model.

Gravity disturbances

Reduced dynamic and *kinematic* accelerations ~~create~~ are used as the input of GEOCOL and are ~~calculated~~ converted to gravity disturbances within that program. These gravity disturbances are ~~declared as~~ the observations.

The gravity disturbances which are derived from EGM96 are on the other hand referred to as predictions. The differences between observations and predictions are presented in figure 7.

The upper map shows how *reduced dynamic* gravity disturbances vary from the reference model while the lower map presents the same comparison with *kinematic* data.

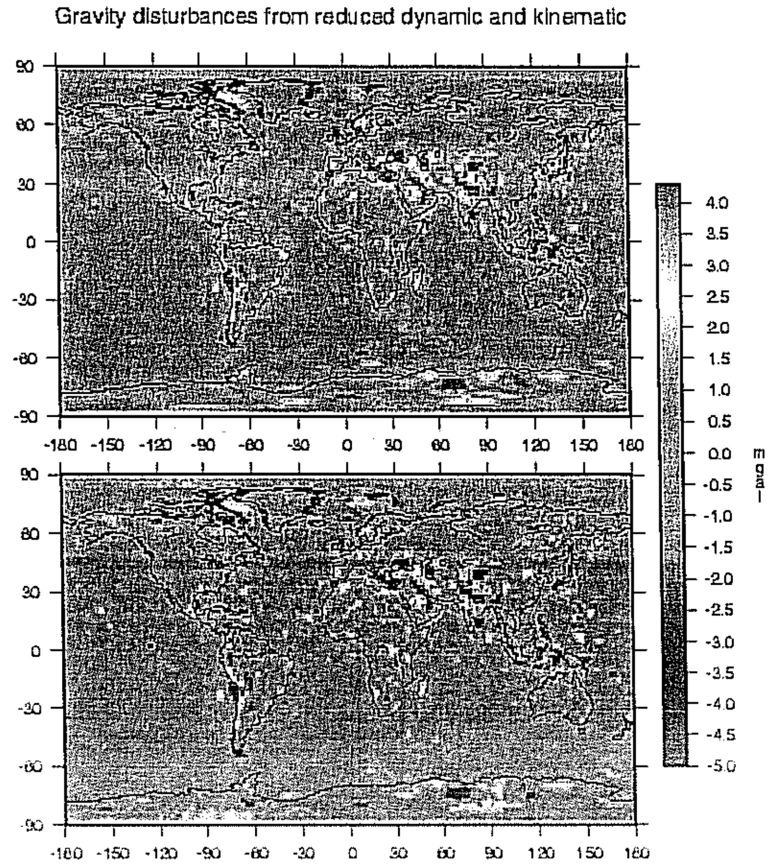

figure 7: gravity disturbances compared to EGM96

Most parts of the maps are green in colour which indicates that the differences lie in between -0.5mgal and 1.5mgal. The *kinematic* data show higher differences than the *reduced dynamic* data. As these differences do not create a specific pattern but are mostly equally spread they are assumed to be noise. Those observations ascertain the results from figure 6.

Both maps of figure 7 have in common that certain areas, such as the Himalayas, Antarctica and the Andes show extreme differences (either around 4mgal or -5mgal). All these specific areas are difficult to access due to topographical reasons. Not many gravity measurements have therefore taken place in those areas. Since this lack of data is reflected in EGM96 it can be assumed that gravity disturbances derived from CHAMP observations are more accurate than from the reference model in those places. Large differences appear as a consequence. Figure 7 ~~encourages~~ confirms the idea that low orbiting satellites are generally able to provide information which would otherwise be very difficult to gain.

Spherical harmonic coefficients

Spherical harmonic coefficients are obtained ~~by~~ using collocation. An important question is now if these coefficients are consistent ~~to~~ with the known. A consistency requires that the standard deviations of coefficient differences (CHAMP – EGM96) are smaller than the standard deviations of the coefficients of EGM96 themselves.

Within an earlier project, a gravity model has been derived by using the energy conservation method [Howe et al. 2003]. Those results should also be verified by the results of this study which is based on the same data set.

In order to judge the results of collocation, figure 8 represents data of the GEOCOL output file. The standard deviation is plotted on the vertical axis while the degree of the coefficients is plotted on the horizontal axis. The standard deviations of coefficients are combined to one standard deviation per degree.

Following graphs are shown (figure 8):

- in red: standard deviations of coefficient differences (*reduced dynamic*-EGM96)
- in blue: standard deviations of coefficient differences (*kinematic*-EGM96)
- in green: standard deviations of coefficients from the energy conservation method
- in brown: standard deviations of coefficients of EGM96
- in cyan: standard deviation of estimated error of *reduced dynamic* coefficients
- in black: standard deviation of estimated error of *kinematic* coefficients

Up to degree 24, EGM96 has been removed from all data (remove-restore technique) therefore the standard deviations of EGM96 initially become zero and the standard deviations of the other data are very small for the first 24 degrees. It is obvious that only the residual standard deviations from degree one to 24 are calculated because only residual coefficients of those degrees are regarded.

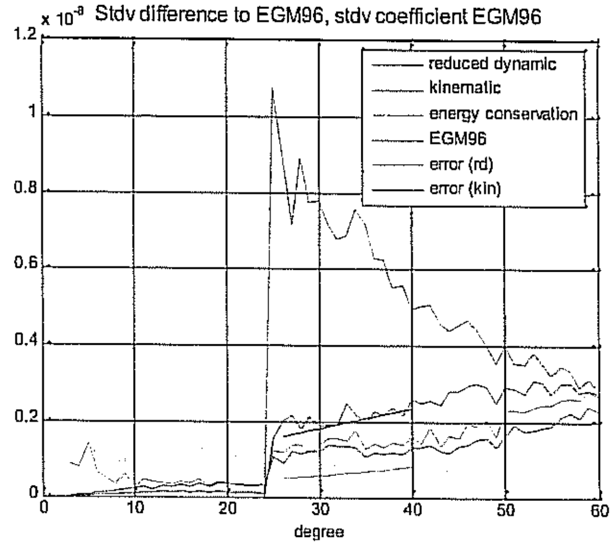

figure 8: comparison of gravity field models

At degree 25 the standard deviation of EGM96 (brown graph) shows its maximum. From that point on, the standard deviations of EGM96 coefficients decreases.

The opposite appears for the difference between EGM96 and CHAMP data (red and blue graph). The higher the degree the more oscillating errors can be observed in the coefficients derived from CHAMP data. As a consequence the standard deviation of differences to EGM96 increases towards higher degrees. However, this increase is slower than the decrease of the standard deviation of EGM96 coefficients (brown graph).

As long as the red and the blue graph are lower than the brown graph, a consistency in comparison to EGM96 is achieved. Calculations are carried out up to degree 60. At this degree, there is an intersection between the blue and brown graph which means that the kinematic data do not give information for a better resolution than 60 degree. The *reduced dynamic* differences, however, are always smaller than the *kinematic* and could as a consequence go a bit further than degree 60.

The results of the energy conservation method (green graph) refer to the *reduced dynamic* data set. Their standard deviations are similar to those derived from accelerations (red graph) but always a bit higher. The energy conservation method has also a noticeable problem with the low degree coefficients. The standard deviations of differences are high in the beginning bearing in mind that EGM96 is removed. This problem does not occur for the graphs based on accelerations (red and blue).

Figure 8 also shows the results of the error estimations of equation 8. In both cases, *reduced dynamic* (cyan) and *kinematic* (black), the standard deviations of the errors are too optimistic in comparison to the evaluated standard deviations of the differences between EGM96 and CHAMP observations.
This can be partly explained by the fact that within the error estimation EGM96 is expected to have a standard deviation of zero while the calculated differences of standard deviations from EGM96 and CHAMP data are influenced by the real standard deviations of EGM96. Asides from these observations, the errors and standard deviations of differences are consistent.

If one takes a closer look at the error estimation of spherical harmonic coefficients that all belong to the same degree, the result will look like figure 9. It shows the errors of coefficients belonging to degree 35 and based on *reduced dynamic* observations. Coefficients of other degrees or based on *kinematic* data result in similar figures.

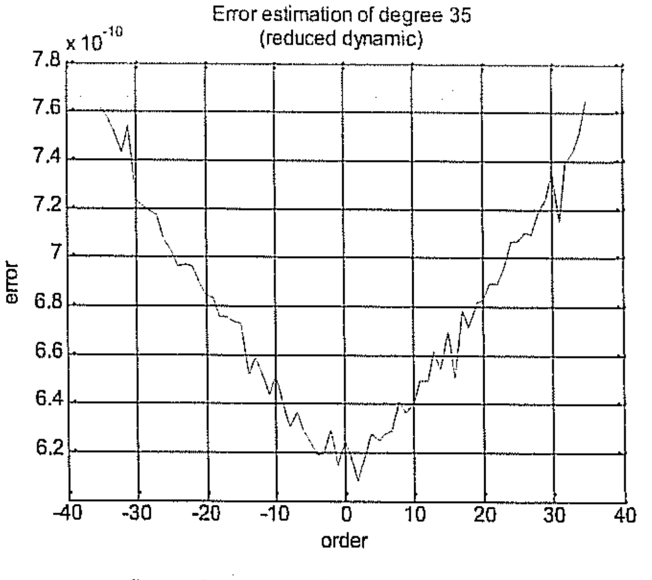

figure 9: error estimation of degree 35

Figure 9 shows that the minimal error occurs around order zero. The higher the magnitude of the order, the more the error increases. This kind of curvature is caused by the lack of satellite measurements in polar regions. Simulations exist which show that the errors of coefficients will present a horizontal line if they are derived from data which are fully distributed over the whole earth. Since CHAMP does not completely cover the poles, one must keep in mind that coefficients of higher orders have higher errors.

How many were used !

CONCLUSION

The main task to calculate a gravity field model using CHAMP data has successfully been carried out. The combination of Newton Interpolation and Least-Squares Collocation presents satisfying results. A reasonable gravity field model up to degree 60 has been created.

The conclusion can be drawn that the computation of spherical harmonic coefficients based on accelerations show an improvement of the gravity field model based on energy conservation.

One has also seen that the *reduced dynamic* data are less influenced by noise than the *kinematic* data if EGM96 is defined as a reference. It is therefore advisable to use the combination of *reduced dynamic* and *kinematic* data during the preprocessing step and then to carry on with only the filtered *reduced dynamic* data set.

However, the above conclusions are only derived from one-third of the observations of one month. More reliable conclusions can be drawn if more observed data are involved.

As the Least-Squares Collocation cannot handle much larger data sets, one possibility is to use Fast Spherical Collocation instead. This requires that the data are converted into gridded values of the same height.

Further investigations accounting for larger data sets should be done to see if similar results, to the one in this study, will be observed and more importantly, if a higher accuracy and resolution of the estimated gravity field model can be achieved.

REFERENCES

[Austen and Reubelt 2000] Austen, G. and Reubelt, T.: Spatial gravity field analysis using semi-continuous ephemerides of low-orbiting GPS-tracked satellites of type CHAMP, GRACE and GOCE. Final Thesis, Institute of Geodesy, University of Stuttgart, http://www.uni-stuttgart.de/gi/education/diplomarbeiten/austen+reubelt.pdf, 2000.

[Howe et al. 2003] Howe, E., Stenseng, L. and Tscherning, C. C.: Analysis of one month of CHAMP state vector and accelerometer data for the recovery of the gravity potential. Advances in Geoscience, 1, 1-4, 2003.

[Lemoine et al. 1998] Lemoine, F., Kenyon, S., Factor, J., Trimmer, R., Pavlis, N., Chinn, D., Cox, C., Klosko, S., Luthcke, S., Torrence, M., Wang, Y., Williamson, R., Pavlis, E., Rapp, R., and Olson, T.: The development of the joint NASA GSFC and the national imagery and mapping agency (NIMA) geopotential model EGM96. Tech. Rep. NASA/TP-1998-206861, NASA Goddard Space Flight Center, 1998.

[Tscherning 1974] Tscherning, C. C.: A FORTRAN IV Program for the Determination of the Anomalous Potential Using Stepwise Least Squares Collocation. Reports of the Department of Geodetic Science No. 212, The Ohio State, University, Columbus, Ohio, 1974.

[Tscherning et al. 1994] Tscherning, C. C., Knudsen, P. and Forsberg, R.: Description of the GRAVSOFT package. Geophysical Institute, University of Copenhagen, Technical Report, http://cct.gfy.ku.dk ,1991, 2. Ed. 1992, 3. Ed. 1993, 4. Ed, 1994.

[Tscherning 2001] Tscherning, C. C.: Computation of spherical harmonic coefficients and their error estimates using Least-Squares Collocation. Journal of Geodesy, 75, 12-18, 2001.

Tin Lian Abt

2004

Differences reduced dynamic − kinematic,
(Tin Lian Abt 2004−10−22)

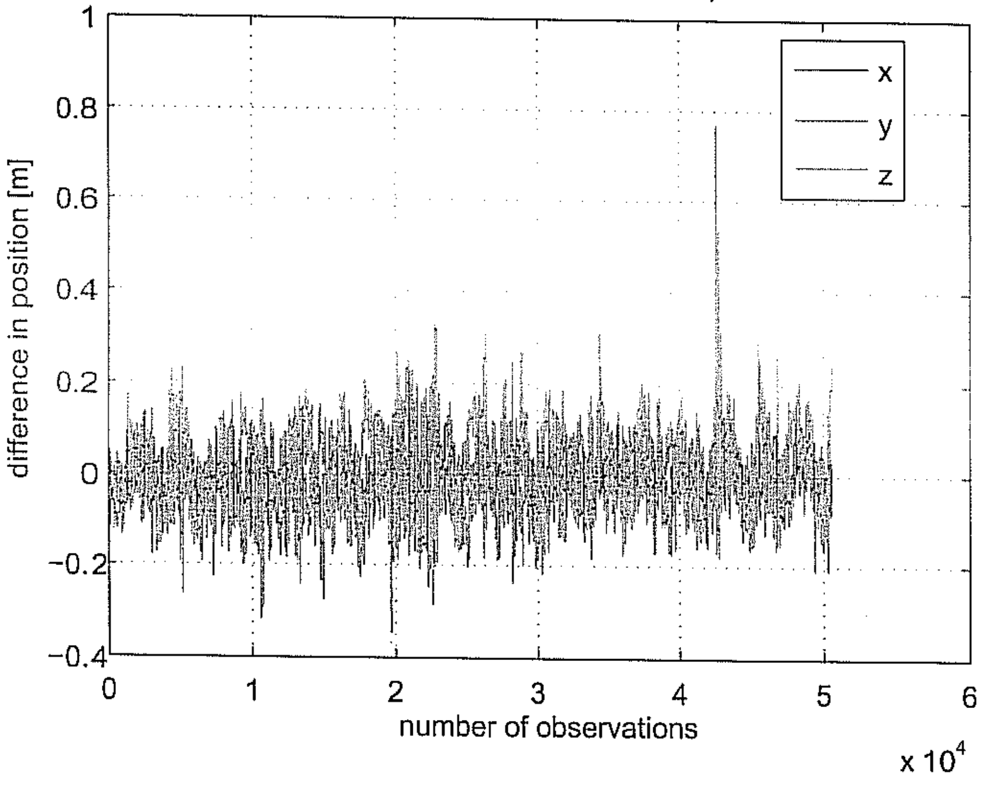

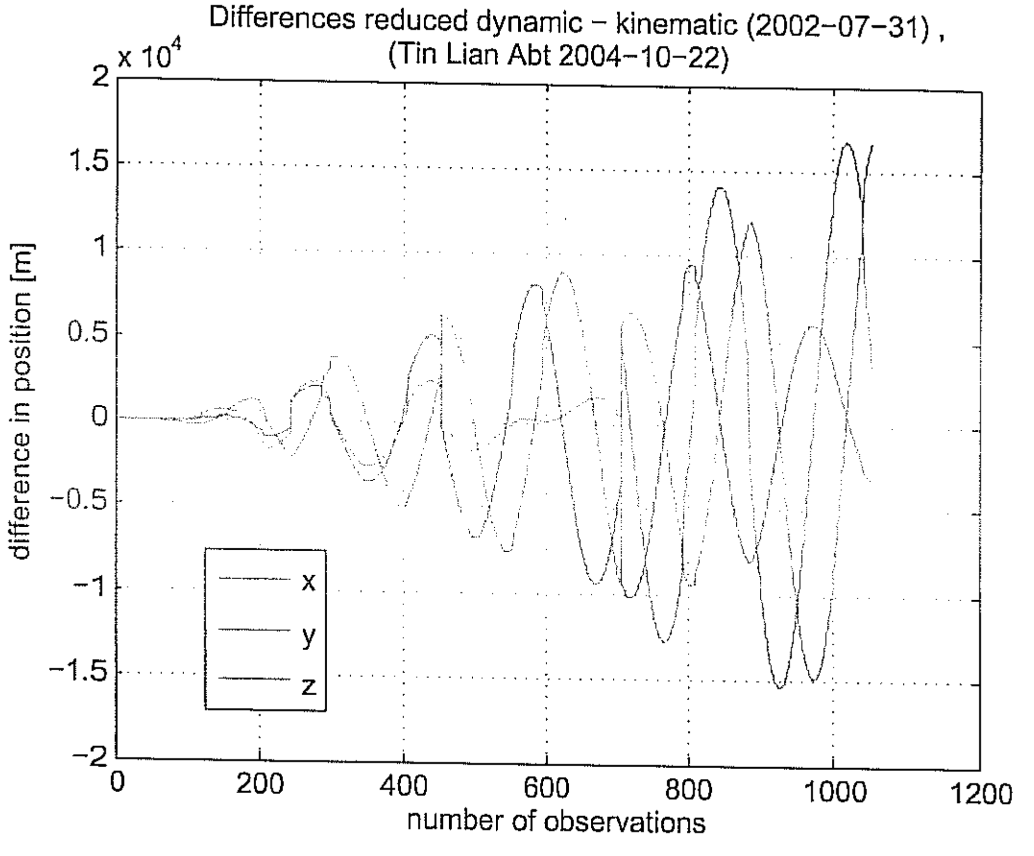

Differences reduced dynamic − kinematic (2002−07−31) ,
(Tin Lian Abt 2004−10−22)
x 10^4
2
1.5
1
0.5
0
−0.5
−1
−1.5
−2
difference in position [m]
0
200
400
600
800
1000
1200
number of observations
x
y
z

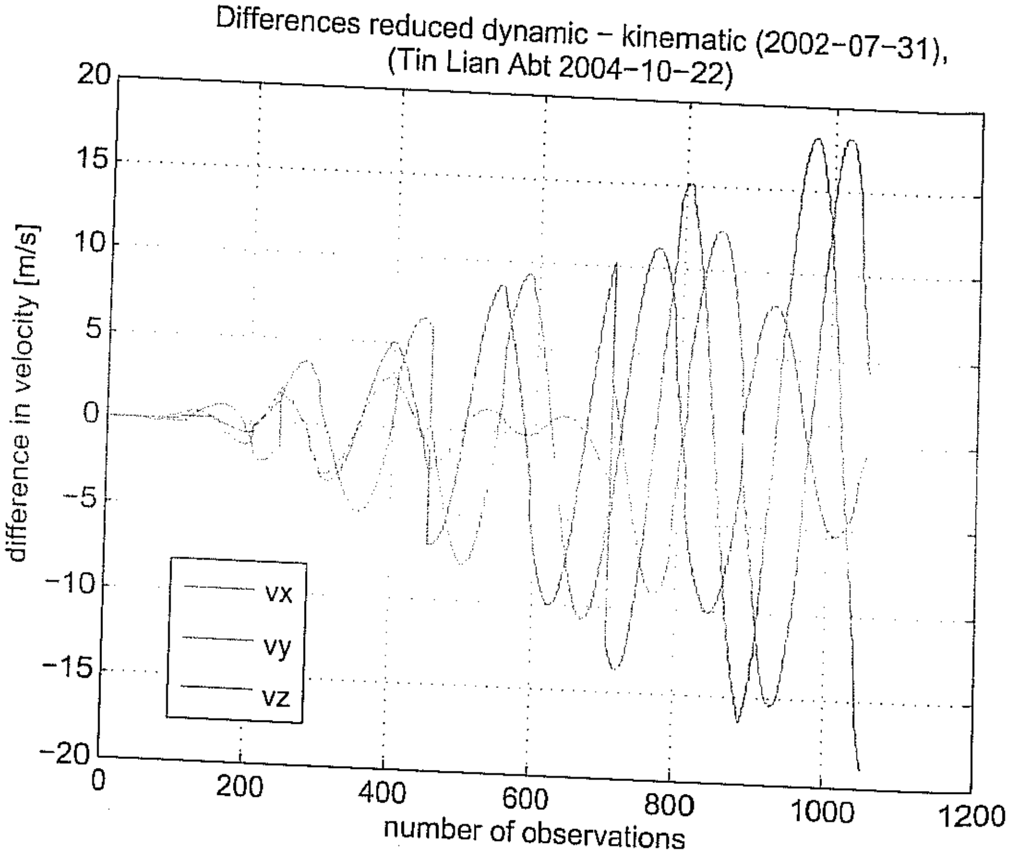
Differences reduced dynamic − kinematic (2002−07−31),
(Tin Lian Abt 2004−10−22)
difference in velocity [m/s]
number of observations
vx
vy
vz
20
15
10
5
0
−5
−10
−15
−20
0
200
400
600
800
1000
1200

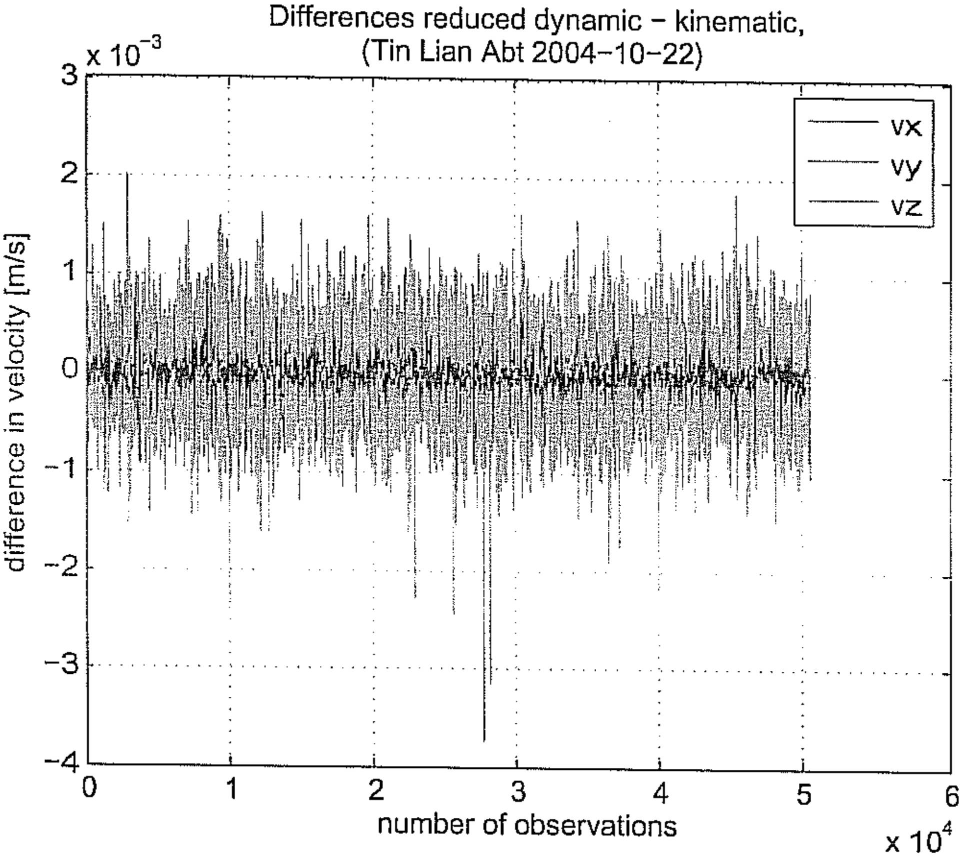

Differences reduced dynamic - kinematic,
(Tin Lian Abt 2004-10-22)
x 10^-3
3
2
1
0
-1
-2
-3
-4
difference in velocity [m/s]
vx
vy
vz
0
1
2
3
4
5
6
number of observations
x 10^4